J. Fluid Mech. (1985), *vol.* 156, *pp.* 39–53
Printed in Great Britain

The approach to self-similarity of the solutions of the shallow-water equations representing gravity-current releases

By R. E. GRUNDY
Mathematical Institute, University of St Andrews, North Haugh, St Andrews KY16 9SS

AND JAMES W. ROTTMAN†
Department of Applied Mathematics and Theoretical Physics, University of Cambridge, Silver Street, Cambridge CB3 9EW

(Received 15 August 1984 and in revised form 3 January 1985)

Known similarity solutions of the shallow-water equations representing the motion of constant-volume gravity currents are studied in both plane and axisymmetric geometries. It is found that these solutions are linearly stable to small correspondingly symmetric perturbations and that they constitute the large-time limits of the solutions of the initial-value problem. Furthermore, the analysis reveals that the similarity solution is approached in an oscillatory manner. Two initial-value problems are solved numerically using finite differences and in each case the approach to the similarity solution is compared with the analytic predictions.

1. Introduction

Gravity currents, which consist of fluid of one density flowing under the influence of gravity into fluid of another density, occur in many natural and industrial situations. Several examples of gravity currents in the atmosphere and the ocean are described in the recent review article by Simpson (1982). One example of current interest is when an industrial storage tank containing a heavier-than-air gas suddenly burst and releases its contents into the atmosphere. Recently the UK Health & Safety Executive has supervised a series of field experiments, McQuaid (1984), that simulates such an accident. The storage tank in the field experiments was a cylinder of circular cross-section with walls made of plastic sheeting. The gas was released by rapidly pulling the sidewalls to the ground with elastic cords. The released gas slumps to the ground producing a gravity current that spreads horizontally. For these types of accidents, particularly if the gas is hazardous, it is important to be able to estimate how rapidly the gravity current spreads over the ground and how this spreading rate is affected by the release conditions.

Theories for the spreading rate of gravity currents owing to the release of a fixed volume of fluid have been proposed by Fay (1969), Fannelop & Waldman (1972) and Hoult (1972). All these theories assume that the buoyancy force driving the current is initially balanced by the inertia. This assumption leads to the result that the length (or radius in axisymmetric flow) increases as $t^{2/(3+n)}$, where $n = 0$ and $n = 1$ for plane and axisymmetric flow respectively, and t is the time after release. Fay (1969) derives

† Present address: Meteorology & Assessment Division, Environmental Sciences Research Laboratory, US Environmental Protection Agency, Research Triangle Park, North Carolina 27711.

this by balancing the force estimates in the current while Fannelop & Waldman (1972) and Hoult (1972) deduce this via similarity solutions of the depth-averaged shallow-water equations.

In the recent laboratory experiments of Huppert & Simpson (1980) and Rottman & Simpson (1983, 1984) gravity currents were produced in both plane and axisymmetric geometries by releasing fixed volumes of salt water in channels filled with fresh water. The results of these experiments show that initially the rate of advance of the gravity current is a strong function of the release conditions, but eventually, if the current does not become so thin that viscous effects become comparable with the inertia of the current, the rate of advance of the current approaches the theoretical result referred to above.

In the present paper, we take a closer look at the similarity solutions originally derived by Fanneløp & Waldman (1972) and Hoult (1972). We want to confirm mathematically that these similarity solutions are the large-time limits of some class of initial-value problems associated with the shallow-water equations. In addition we want to obtain some indication of how rapidly these similarity solutions are approached and how sensitive this rate of approach is to the initial conditions.

We do this in two ways. First we construct a large-time asymptotic expansion with the similarity solution as the leading term – a procedure which also serves as a linear stability analysis for symmetric disturbances. As we shall see later, this results in a linear eigenvalue problem possessing an infinite discrete spectrum of eigenvalues $\{\lambda_i\}$. These determine the rate at which the similarity solution is approached as $t \to \infty$ and, since $\mathrm{Re}\,(\lambda_i) < 0$ for all λ_i, confirms linear stability. As a second confirmation of the large-time behaviour, we solve numerically the 'dam-break' initial-value problem for both plane and axisymmetric geometries. An important facet of our work is the subsequent comparison between the numerical solutions and the analytic predictions.

The problem is formulated in §2. The similarity solutions are written down in §3 and the linear eigenvalue problem associated with the large-time expansion is derived and solved in §4. The numerical methods used to solve the 'dam-break' problem are outlined and the results of the computations are described and compared with the asymptotic results in §5. The results are summarized and further discussed in §6.

2. Formulation of the problem

We consider the plane and axisymmetric motion under the influence of gravity of a finite volume of fluid with density ρ that is released from rest on the horizontal bottom boundary of another fluid with slightly lower density ρ_a. The two fluids are assumed to be incompressible and miscible (so that surface-tension effects are unimportant) and any mixing between them is neglected. A sketch of the flow defining the nomenclature and coordinate system is shown in figure 1.

If the thickness of the heavy-fluid layer is small compared with its length and with the depth of the surrounding fluid and if viscous effects are unimportant, then the motion of the heavy fluid is described approximately by the shallow-water equations, as derived (for example) by Penney & Thornhill (1952):

$$\frac{\partial h}{\partial t} + u\frac{\partial h}{\partial x} + h\frac{\partial u}{\partial x} + n\frac{uh}{x} = 0, \tag{2.1}$$

$$\frac{\partial u}{\partial t} + u\frac{\partial u}{\partial x} + g'\frac{\partial h}{\partial x} = 0. \tag{2.2}$$

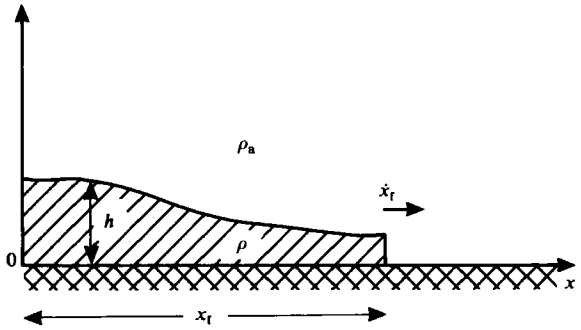

FIGURE 1. Schematic illustration of a heavy fluid with density ρ spreading at the base of a lighter fluid of density ρ_a. The position of the front of the spreading current is denoted by $x_f(t)$.

Here $h(x, t)$ is the thickness of the heavy fluid, $u(x, t)$ is the depth-averaged horizontal fluid speed and $g' = g(\rho-\rho_a)/\rho_a$ is the reduced acceleration due to gravity. Note that we have used the Boussinesq approximation to replace ρ in the denominator of this expression for g' by ρ_a. The independent variable x represents the horizontal coordinate in plane flow and the radial coordinate in axisymmetric flow. The independent variable t represents the time, which is zero when the heavy fluid is released. The parameter n is zero for plane flow and unity for axisymmetric flow.

Equations (2.1) and (2.2) are hyperbolic and can be written in the characteristic form

$$h\frac{\mathrm{d}u}{\mathrm{d}t}\pm c\frac{\mathrm{d}h}{\mathrm{d}t}\pm nc\frac{uh}{x}=0, \tag{2.3}$$

along the characteristic curves specified by

$$\frac{\mathrm{d}x}{\mathrm{d}t}=u\pm c, \tag{2.4}$$

where

$$c=(g'h)^{\frac{1}{2}}.$$

We impose the boundary conditions

$$u(0, t)=0, \tag{2.5}$$

$$u(x_f, t)=\dot{x}_f, \tag{2.6}$$

$$\beta^2 g' h(x_f, t)=\dot{x}_f^2, \tag{2.7}$$

where the function $x_f(t)$ denotes the position of the front of the heavy fluid and $\dot{x}_f(t)$ is its speed. Boundary condition (2.5) implies that no fluid enters the current from the plane or axis of symmetry at $x = 0$, and (2.6) implies that no fluid enters the current at the front. Boundary condition (2.7) represents a quasi-steady balance between the buoyancy force driving the current front and the drag on the front due to its acceleration of the surrounding fluid. The buoyancy force driving the current front is proportional to $g(\rho-\rho_a)h_f^2$, where $h_f = h(x_f, t)$, and the drag due to the surrounding fluid is proportional to $\rho_a h_f \dot{x}_f^2$. If the acceleration of the front is small, then these two forces must approximately balance. Equating these two forces, we obtain (2.7), where β is a function of the constants of proportionality. It is found experimentally that β is about unity for currents with small values of $(\rho-\rho_a)/\rho_a$. This front condition is necessary in our formulation because it is observed that

vertical accelerations are not small at the current front and therefore the shallow-water equations are invalid there. Boundary conditions (2.6) and (2.7) are analogous to shock conditions in gasdynamics. For gravity-current flows, these boundary conditions have been used by all the investigators mentioned in the introduction.

Integrating (2.1) with respect to x over $[0, x_f(t)]$ and using (2.5) and (2.6), we obtain the integral invariant

$$\int_0^{x_f(t)} h(x, t)\,(2\pi x)^n \,\mathrm{d}x = Q, \tag{2.8}$$

where Q is the volume of the heavy fluid (volume per unit width for plane flow). This shows that the volume of the heavy fluid is conserved.

To complete the problem, we need to specify the initial conditions. In general, for the problems in which we are interested here

$$h(x, 0) = \begin{cases} h_0(x), & 0 \leqslant x \leqslant x_0, \\ 0, & x_0 < x, \end{cases} \tag{2.9}$$

$$u(x, 0) = 0, \tag{2.10}$$

with

$$x_f(0) = x_0. \tag{2.11}$$

In §5, we consider the particular initial conditions for which $h_0(x) = h_0$ (a constant) in both plane and axisymmetric geometries.

3. Similarity solutions

Inspection of (2.1) to (2.11) shows that $h(x, t)$ can be replaced by $g'h(x, t)$. Then the five governing parameters in the problem are t, $(g'Q)$, x, x_0, and β. Since there are two independent dimensions (length and time) the problem can be expressed in terms of three dimensionless parameters, which we choose to be

$$\xi = x(g'Q)^{-1/(3+n)}\, t^{-2/(3+n)}, \quad \tau = t(g'Q)^{\frac{1}{2}} x_0^{-(3+n)/2} \tag{3.1, 3.2}$$

and β. The parameter ξ may be thought of as a dimensionless space variable and τ as a dimensionless time variable, scaled by a time characteristic of the initial conditions. The dependent variables may then be expressed as:

$$g'h(x, t) = (g'Q)^{2/(3+n)}\, t^{-2(1+n)/(3+n)}\, H(\xi, \tau, \beta); \tag{3.3}$$

$$u(x, t) = (g'Q)^{1/(3+n)}\, t^{-(1+n)/(3+n)}\, U(\xi, \tau, \beta); \tag{3.4}$$

$$x_f(t) = (g'Q)^{1/(3+n)}\, t^{2/(3+n)}\, A(\tau, \beta); \tag{3.5}$$

where H, U and A are dimensionless functions.

We now substitute (3.3)–(3.5) into (2.1) and (2.2) and seek solutions for H, U and A that are independent of τ. If such solutions exist that satisfy the boundary conditions (2.5)–(2.7) then the problem is said to possess a similarity (or self-similar) solution. This solution will not, in general, satisfy the initial conditions but, if stable to small disturbances, we expect it to be the limiting form as $\tau \to \infty$ of the solution of the initial-value problem for a wide class of initial conditions. We note from (3.5) that the similarity solution has the observed large-time spreading behaviour.

The similarity solutions are well known from gas dynamics and can be written, with $\eta = \xi/A_0$, as

$$A(\tau) = A_0, \tag{3.6}$$

$$H \equiv H_0 = \frac{(n+1)A_0^2}{(n+3)^2}(\eta^2+B), \tag{3.7}$$

$$U \equiv U_0 = \frac{2A_0\eta}{n+3}, \tag{3.8}$$

with

$$B = \frac{4}{(n+1)\beta^2} - 1. \tag{3.9}$$

In the gas-dynamic context the family of similarity solutions of which (3.7) and (3.8) are a special case were first studied by Guderley (1942). This powerful phase-plane approach was further developed by Courant & Friedrichs (1948) and Sedov (1956) with refinements by many subsequent authors. Using the phase-plane method it is not difficult to show that (3.6)–(3.9) with (3.3)–(3.5) constitute for $0 < \beta < 2/(n+1)^{\frac{1}{2}}$ the unique similarity solution to (2.1), (2.2), (2.5)–(2.7) with A_0 determined by the mass-invariance condition (2.8) to give

$$A_0 = \left\{\frac{(n+1)(n+3)^3\beta^2}{(2\pi)^n[4(n+3)-2(n+1)\beta^2]}\right\}^{1/(n+3)}. \tag{3.10}$$

For $\beta \geqslant 2/(n+1)^{\frac{1}{2}}$ a similarity solution satisfying the boundary and mass invariance conditions does not exist. The above solution is, written in a necessarily different form, identical with that of Hoult (1972).

4. Approach to self-similarity

We now consider how the similarity solutions are approached as $\tau \to \infty$. For this purpose, we investigate the possibility that $H(\eta, \tau)$, $U(\eta, \tau)$ and $A(\tau)$ can be expanded in the form

$$H(\eta, \tau) = H_0(\eta) + \sum_j \tau^{\mu_j} H_j(\eta), \tag{4.1}$$

$$U(\eta, \tau) = U_0(\eta) + \sum_j \tau^{\mu_j} U_j(\eta), \tag{4.2}$$

$$A(\tau) = A_0\left\{1 + \sum_j \tau^{\mu_j} A_j\right\}, \tag{4.3}$$

in the limit $\tau \to \infty$, $\eta = O(1)$. The functions H_0, U_0 and the parameter A_0 are similarity solutions (3.7), (3.8) and (3.10).

The choice of power-law perturbations is the only possible one, consistent with related problems in other fields (see Stewartson & Thompson 1968), so a necessary condition for the expansions (4.1)–(4.3) to exist is that Re $(\mu_j) < 0$. We will prove this result later in the paper. The correction terms to the similarity solutions that arise in (4.1)–(4.3) are of three types. The first, the so-called linear perturbations, are found by solving a linear eigenvalue problem for μ_j. We denote the μ_j determined in this way by γ_j. The second type are generated by the nonlinear self-interactions of the first type and satisfy second-order linear boundary-value problems. A third type

may exist when the power of τ in an interaction term equals one of the γ_j; in this event logarithms may be involved. In this paper we concern ourselves with the first type of perturbation and the values $\{\gamma_j\}$ are called the eigenvalues of the similarity solutions.

It turns out that the γ_j form a discrete spectrum in the complex plane, occurring in conjugate pairs. Once the sequence $\{\gamma_j\}$ has been found, then the eigenvalue with the largest real part constitutes the dominant correction to the similarity solution, while all possible products generate the interaction terms. Finally, if $\mathrm{Re}\,(\gamma_j) < 0$, which as we shall see is true, then the similarity solution is linearly stable with respect to small symmetric disturbances.

We formally substitute (4.1) and (4.2) into equations (2.1), using (3.3) and (3.4), and equate powers of τ^{γ_j}. The resulting equation for $H_j(\eta)$ can be written

$$[(\eta^2+B)\,\eta^n H_j']' + \frac{3+n}{1+n}[\gamma_j(n-1)-\gamma_j^2(n+3)]\,\eta^n H_j = 0, \tag{4.4}$$

where $H_j(\eta)$ and $U_j(\eta)$ are related by

$$U_j(\eta) = -\frac{(n+3)\,H_j'(\eta)}{A_0[\gamma_j(n+3)-(n-1)]}, \tag{4.5}$$

and primes denote differentiation with respect to η. Substituting (4.1)–(4.3) into the boundary conditions (2.5)–(2.7), using (3.3)–(3.5), we find that to $O(\tau^{\gamma_j})$ (2.5) gives

$$H_j'(0) = 0, \tag{4.6}$$

while (2.6) gives

$$A_j = -\frac{(n+3)^2\,H_j'(1)}{A_0^2[(n+3)\,\gamma_j-(n-1)]\,(n+3)\,\gamma_j}, \tag{4.7}$$

and (2.7) yields

$$[2(n+3)\,\gamma_j+4-(n+1)\,\beta^2]\,H_j'(1)-\tfrac{1}{2}(n+3)\,\beta^2\gamma_j[(n-1)-\gamma_j(n+3)]\,H_j(1) = 0. \tag{4.8}$$

Since the equations and boundary conditions (4.4)–(4.8) are linear and homogeneous then the solution will determine γ_j together with H_j, U_j and A_j to within an arbitrary constant factor.

At this stage we can show that $\mathrm{Re}\,(\gamma_j) < 0$. Taking the complex conjugate of (4.4), multiplying by $\frac{1}{2}\gamma_j(n+3)\,\beta^2[(n-1)-\gamma_j(n+3)]\,H_j$, integrating over [0, 1] and using (4.6) and (4.8), we obtain a quadratic expression for each γ_j with coefficients that are real and positive for any complex γ_j (for $n = 0$ or 1). To be specific, we find that

$$\gamma_j^2 + D(\gamma_j)\,\gamma_j + E(\gamma_j) = 0, \tag{4.9}$$

where

$$D(\gamma_j) = \frac{16\,|H_j'(1)|^2+\beta^2(1-n^2)\int_0^1 (\eta^2+B)\,\eta^n\,|H_j'|^2\,\mathrm{d}\eta}{(1+n)\,(3+n)\,\beta^4\int_0^1 (\eta^2+B)\,\eta^n\,|H_j'|^2\,\mathrm{d}\eta}, \tag{4.10}$$

and

$$E(\gamma_j) = \frac{8[4-\beta^2(n+1)]+2(n+1)\,\beta^2\,|\gamma_j(n-1)-\gamma_j^2(n+3)|^2\int_0^1 \eta^n\,|H_j|^2\,\mathrm{d}\eta}{(1+n)\,(3+n)^2\,\beta^4\int_0^1 (\eta^2+B)\,\eta^n\,|H_j'|^2\,\mathrm{d}\eta}. \tag{4.11}$$

We therefore conclude that $\mathrm{Re}\,(\gamma_j) < 0$, and that the similarity solutions are stable to linear perturbations.

To proceed further with the solution, we note that (4.4) is easily transformed into the hypergeometric equation, and the solution that satisfies (4.6) is

$$H_j = K_j F(a, b; \tfrac{1}{2}(n+1); -\eta^2/B), \tag{4.12}$$

where

$$a+b = \tfrac{1}{2}(n+1), \quad ab = \frac{\gamma_j(n+3)\,[(n-1)-\gamma_j(n+3)]}{4(n+1)}. \tag{4.13, 4.14}$$

The K_j are arbitrary complex constants and $F(a, b; c; z)$ is the hypergeometric function. Substituting (4.12) into (4.8), we obtain the equation for the eigenvalues, viz

$$F\left(a, a; \tfrac{1}{2}(n+1); \beta^2\frac{n+1}{4}\right) + \left[\frac{2\gamma_j(n+3)+4-\beta^2(n+1)}{2(n+1)}\right] F\left(a+1, a; \tfrac{1}{2}(n+3); \beta^2\,\frac{n+1}{4}\right) = 0. \tag{4.15}$$

The transformation to argument $\frac{1}{4}\beta^2(n+1)$ has been made so that the hypergeometric functions can be computed using their series representation within their radii of convergence, since $0 < \beta^2 < 4/(n+1)$. The eigenvalues, occurring in conjugate pairs, that satisfy this equation must be determined numerically. The associated eigenfunctions are given by (4.12) with the K_j remaining arbitrary and determined in some way by the initial conditions.

Finally, it is interesting and profitable to solve the eigenvalue problem using the Liouville–Green (or WKB) method, ostensibly a large-$|\gamma|$ solution. The straightforward solution is singular, but this difficulty can be overcome using matched expansions. The result of this calculation gives the eigenvalues

$$\gamma \sim \gamma_\infty = -\tfrac{1}{2} + \frac{2\pi i m}{3[\log(2+\beta) - \log(2-\beta)]}, \tag{4.16}$$

with $m = \pm 1, \pm 2, \ldots$ for $n = 0$, and

$$\gamma \sim \gamma_\infty = \frac{\{-[\log(2+\beta) - \log(2-\beta)] + i\pi m\}}{2\sqrt{2}\,[\log(\sqrt{2}+\beta) - \log(\sqrt{2}-\beta)]} \tag{4.17}$$

with $m = \pm 1, \pm 2, \ldots$ for $n = 1$.

The results of the eigenvalue calculations are shown in tables 1 and 2. In table 1 the real and imaginary parts of the first eleven eigenvalues, when conjugates are included, are listed for $n = 0$ and $\beta = 0.6\,(0.2)\,1.4$, together with the Liouville–Green result. The imaginary-part differences clearly indicate the utility of this result in spacing the eigenvalues along $\mathrm{Re}\,(\gamma_m) = -0.5$ for all but the first few values. In table 2 we display the corresponding information for $n = 1$, $\beta = 0.4\,(0.2)\,1.2$. The increasing accuracy of the Liouville–Green result for $\mathrm{Re}\,(\gamma)$ and $\mathrm{Im}\,(\gamma)$ as $\mathrm{Im}\,(\gamma)$ increase is evident. The $\mathrm{Re}\,(\gamma_m)$ are weak functions of m and β and in all cases shown in the table are located at about $\mathrm{Re}\,(\gamma_m) \approx -0.2$. Since $\mathrm{Re}\,(\gamma_m)$ is independent of m for $n = 0$ and weakly dependent on m for $n = 1$, we conclude that the asymptotic rate of approach to similarity is fairly insensitive to the initial conditions. The eigenvalue $\gamma = -1$, which occurs for both values of n, has a simple interpretation. Since the similarity solutions have an arbitrary time origin, τ can be replaced by $\tau_1 + \tau_0$, where τ_0 is a constant. If the similarity solutions are then expanded for large

$n = 0$

$\beta = 0.6$			$\beta = 0.8$			$\beta = 1.0$			$\beta = 1.2$			$\beta = 1.4$		
Exact			Exact			Exact			Exact			Exact		
Re (γ)	Im (γ)	Δ Im (γ)	Re (γ)	Im (γ)	Δ Im (γ)	Re (γ)	Im (γ)	Δ Im (γ)	Re (γ)	Im (γ)	Δ Im (γ)	Re (γ)	Im (γ)	Δ Im (γ)
−1.0	0.0		−1.0	0.0		−1.0	0.0		−1.0	0.0		−1.0	0.0	
		3.323			2.795			1.803			1.384			1.056
−0.5	3.323		−0.5	2.795		−0.5	1.803		−0.5	1.384		−0.5	1.056	
		3.414			2.901			1.960			1.577			1.288
−0.5	6.737		−0.5	5.696		−0.5	3.763		−0.5	2.961		−0.5	2.344	
		3.393			2.877			1.923			1.531			1.231
−0.5	10.130		−0.5	8.573		−0.5	5.686		−0.5	4.492		−0.5	3.575	
		3.388			2.872			1.915			1.521			1.220
−0.5	13.518		−0.5	11.445		−0.5	7.601		−0.5	6.013		−0.5	4.795	
		3.387			2.869			1.911			1.517			1.214
−0.5	16.905		−0.5	14.314		−0.5	9.512		−0.5	7.530		−0.5	6.009	
Liouville–Green			Liouville–Green			Liouville–Green			Liouville–Green			Liouville–Green		
−0.5	3.383 m		−0.5	2.866 m		−0.5	1.906 m		−0.5	1.511 m		−0.5	1.207 m	

TABLE 1. The first eleven eigenvalues (including complex conjugates) for $n = 0$, $\beta = 0.6(0.2)1.4$ listed in order of increasing imaginary part. The third column in each entry gives the difference between successive imaginary parts. The Liouville–Green result is also given with $m = 0, \pm 1, \pm 2, \ldots$.

$n = 1$

$\beta = 0.4$			$\beta = 0.6$			$\beta = 0.8$			$\beta = 1.0$			$\beta = 1.2$		
Exact			Exact			Exact			Exact			Exact		
Re (γ)	Im (γ)	Δ Im (γ)	Re (γ)	Im (γ)	Δ Im (γ)	Re (γ)	Im (γ)	Δ Im (γ)	Re (γ)	Im (γ)	Δ Im (γ)	Re (γ)	Im (γ)	Δ Im (γ)
−1.0	0.0		−1.0	0.0		−1.0	0.0		−1.0	0.0		−1.0	0.0	
		4.627			2.945			2.054			1.472			1.025
−0.244	4.627		−0.235	2.945		−0.220	2.054		−0.197	1.472		−0.155	1.025	
		3.886			2.506			1.782			1.305			0.921
−0.246	8.513		−0.240	5.451		−0.230	3.836		−0.213	2.777		−0.183	1.946	
		3.845			2.474			1.751			1.278			0.903
−0.246	12.358		−0.241	7.925		−0.232	5.587		−0.217	4.055		−0.190	2.849	
		3.833			2.463			1.743			1.270			0.897
−0.246	16.191		−0.241	10.388		−0.233	7.330		−0.218	5.325		−0.192	3.746	
		3.829			2.459			1.738			1.266			0.893
−0.246	20.020		−0.241	12.847		−0.233	9.068		−0.219	6.591		−0.194	4.639	
Liouville–Green			Liouville–Green			Liouville–Green			Liouville–Green			Liouville–Green		
−0.247	3.82 m		−0.242	2.453 m		−0.234	1.732 m		−0.220	1.26 m		−0.196	0.888 m	

TABLE 2. The first eleven eigenvalues (including complex conjugates) for $n = 1$, $\beta = 0.4(0.2)1.2$ listed in order of increasing imaginary part. The third column in each entry gives the difference between successive imaginary part. The Liouville–Green result is also given with $m = 0, \pm 1, \pm 2, \ldots$.

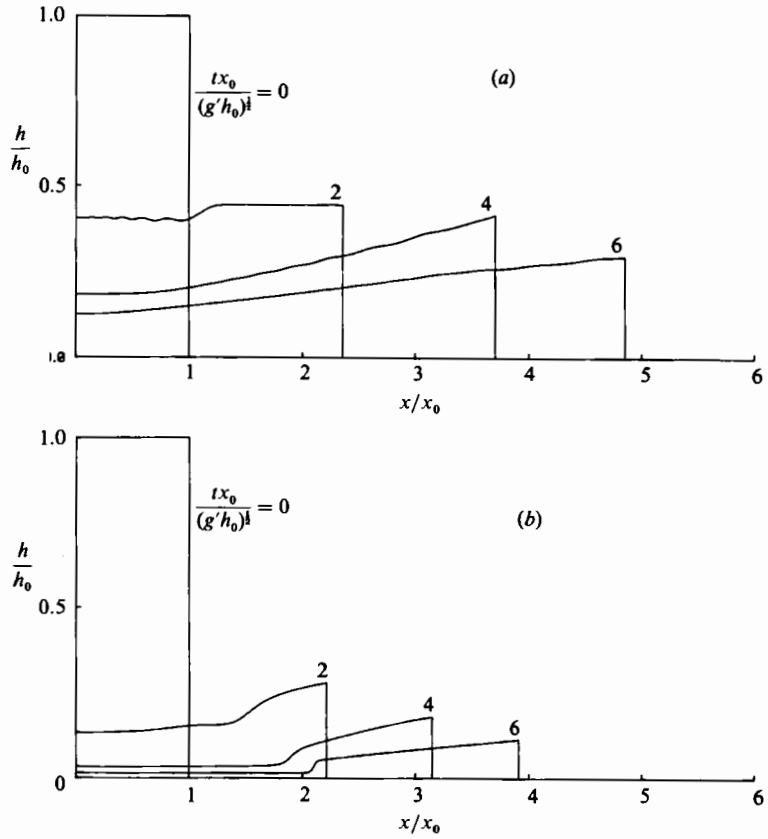

FIGURE 2. The computed height profile $h(x, t)$ of the heavy fluid for several times just after release for the 'dam-break' problem: (*a*) plane ($n = 0$), (*b*) axisymmetric ($n = 1$).

τ_1, the original similarity solutions are obtained as functions of τ_1 along with a correction of $O(\tau_1^{-1})$.

5. Numerical solutions

In this section we describe the numerical solutions of two initial-value problems associated with (2.1) and (2.2). The problems we consider have the initial conditions given by (2.9)–(2.11) with $h_0(x) = h_0$, a constant, for both plane and axisymmetric flow. These are the initial conditions for the classical 'dam-break' problem, as described by Stoker (1957), but the front boundary condition (2.7) makes our problem different from the classical one. Numerical solutions of the 'dam-break' problem, in which the current depth vanishes at the front, are described by Penney & Thornhill (1952), for both plane and axisymmetric flows.

Rottman & Simpson used the method of characteristics to solve the plane-flow problem (1983) and the axisymmetric problem (1984) posed here. The solutions they obtained for the height $h(x, t)$ of the heavy fluid for early times after release are shown in figure 2. The solutions for the two geometries are significantly different, somewhat surprisingly since the similarity solutions are almost identical (apart from a time-dependent scaling factor). The plane solution shows the mound of heavy fluid collapsing almost as a rectangular box, whereas the axisymmetric solution shows that

most of the heavy fluid is, by $t \approx 4x_0/(g'h_0)^{\frac{1}{2}}$, concentrated at the leading edge of the spreading current. In fact, a backward-facing hydraulic jump forms just behind the front at $t \approx 2x_0/(g'h_0)^{\frac{1}{2}}$ and propagates back towards the axis of symmetry.

For large times after release the current becomes very thin and any numerical method would become prone to round-off error. Therefore, to determine the large-time behaviour of these problems and to compare the behaviour with the similarity solutions, we found it more convenient to reformulate the problem in terms of the dependent variables H and U defined by (3.3) and (3.4) and the independent variables η, defined by (3.7), and

$$T = \frac{1}{A_0}\log\tau, \tag{5.1}$$

where τ is given by (3.2) and A_0 by (3.18). This choice of variables keeps the independent variable within reasonable ranges while the dependent variables can be compared directly with the similarity forms. The governing equations (2.1) and (2.2), now become

$$\frac{\partial H}{\partial T} + \tilde{U}\frac{\partial H}{\partial \eta} + H\frac{\partial \tilde{U}}{\partial \eta} + n\frac{\tilde{U}H}{\eta} = 0, \tag{5.2}$$

$$\frac{\partial \tilde{U}}{\partial T} + \tilde{U}\frac{\partial \tilde{U}}{\partial \eta} + \frac{\partial H}{\partial \eta} = [\tfrac{1}{2}(n-1)\,\tilde{U} + \tfrac{1}{2}(n+1)\,U_0]\frac{U_0}{\eta}, \tag{5.3}$$

where

$$\tilde{U} = U - U_0, \tag{5.4}$$

and U_0 is the similarity solution given by (3.15). These hyperbolic equations can be written in the characteristic form

$$H\frac{\mathrm{d}\tilde{U}}{\mathrm{d}t} \pm C\frac{\mathrm{d}H}{\mathrm{d}T} \pm nC\frac{\tilde{U}H}{\eta} = [\tfrac{1}{2}(n-1)\,\tilde{U} + \tfrac{1}{2}(n+1)\,U_0]\frac{U_0 H}{\eta}, \tag{5.5}$$

along the characteristic curves specified by

$$\frac{\mathrm{d}\eta}{\mathrm{d}T} = \tilde{U} \pm C, \tag{5.6}$$

where $C = H^{\frac{1}{2}}$. The boundary conditions (2.5)–(2.7) become

$$\tilde{U}(0, T) = 0, \tag{5.7}$$

$$\tilde{U}(\eta_f, T) = \frac{\mathrm{d}\eta_f}{\mathrm{d}T}, \tag{5.8}$$

$$\beta^2 H(\eta_f, T) = [\tilde{U}(\eta_f, T) + U_0(\eta_f)]^2, \tag{5.9}$$

where

$$\eta_f(T) = \frac{A(T)}{A_0} \tag{5.10}$$

is the value of η at the front.

We used an explicit finite-difference scheme to solve (5.2) and (5.3) with boundary conditions (5.7)–(5.9). Specifically, a Lax–Wendroff method was used along with a flux-corrected transport algorithm as described by Book, Boris & Hain (1975). The flux-correction technique was necessary to compute accurately the hydraulic jump that occurs in the axisymmetric problem. The values of the dependent variables at the boundaries $\eta = 0$ and $\eta = \eta_f(T)$ as well as the value of $\eta_f(T)$ were determined from (5.7)–(5.9) and from solving first-order finite-difference representations of (5.5) along

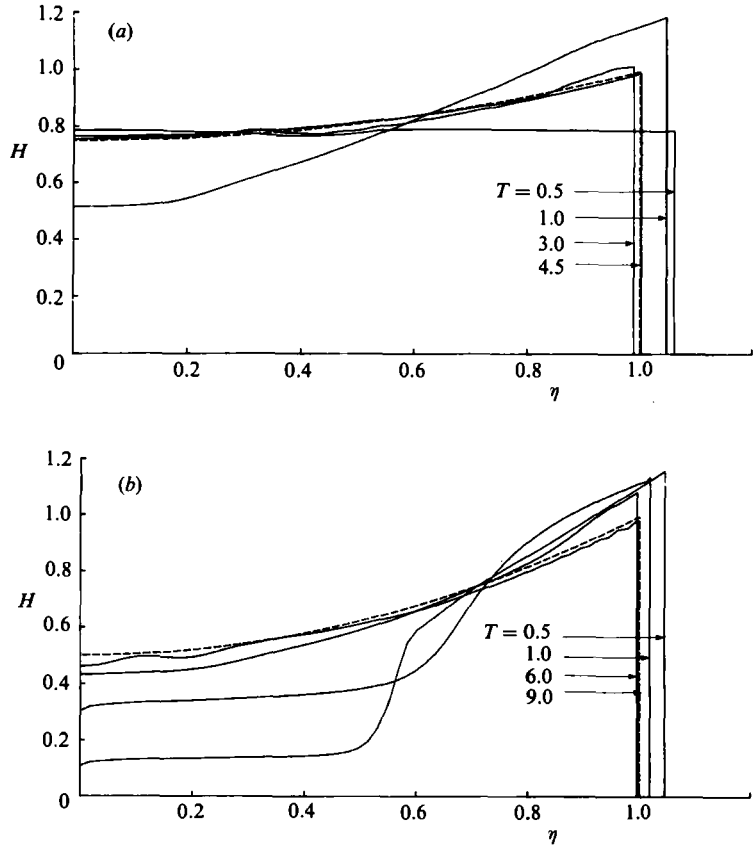

FIGURE 3. The computed height profiles $H(\eta, T)$ for several values of the dimensionless time T after release for the 'dam-break' problem: (*a*) plane ($n = 0$), (*b*) axisymmetric ($n = 1$). The dashed curve in each plot is the similarity solution $H_0(\eta)$.

backward- and forward-moving characteristic lines, respectively. As initial conditions, we used the results of the characteristic calculations by Rottman & Simpson (1983, 1984).

Results of the numerical calculations for the case with $\beta = 1$ are shown in figures 3 and 4. Figures 3(*a*) and 3(*b*) are plots of $H(\eta, T)$ at several values of T for $n = 0$ and 1, respectively. Figures 4(*a*) and 4(*b*) are plots of the front position $\eta_f(T)$ as a function of T for the two geometries. In both figures the similarity solutions are shown as dashed curves. It is clearly seen that the numerical results oscillate in time as they approach the similarity solution with the amplitudes of the oscillations decreasing rapidly with T. By the time $T \approx 6$ (for $n = 0$) and $T \approx 10$ (for $n = 1$) the numerical solutions are equal to the similarity solution to within the accuracy of the calculation.

This damped-oscillatory approach to the similarity solution is anticipated by the analytical results obtained in §4. For example, from (4.3) and (5.10) it is seen that, in terms of the transformed time T,

$$\eta_f(T) = 1 + \sum_j \exp\left[\mathrm{Re}\,(\gamma_j)\, A_0\, T\right]\{a_j \cos\left[\mathrm{Im}\,(\gamma_j)\, A_0\, T\right] + b_j \sin\left[\mathrm{Im}\,(\gamma_j)\, A_0\, T\right]\}, \tag{5.11}$$

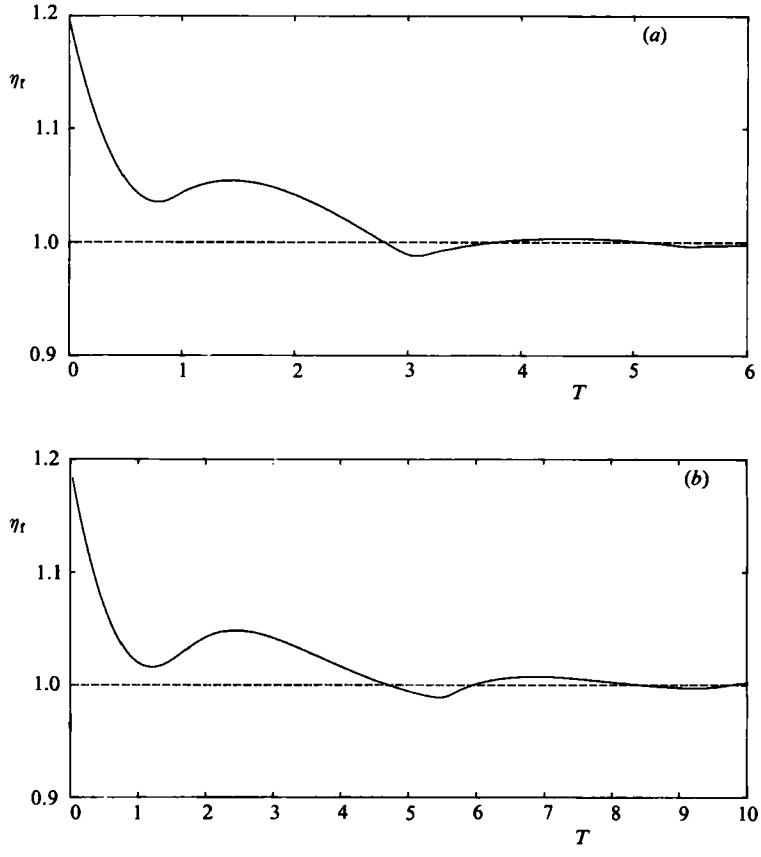

FIGURE 4. The computed transformed front position $\eta_f(T)$ for the 'dam-break' problem: (*a*) plane ($n = 0$), (*b*) axisymmetric ($n = 1$). The dashed line in each plot is $\eta_f(T) = 1$, the value predicted by the similarity solution.

since the γ_j always appear in conjugate pairs. The coefficients a_j and b_j are real constants that depend in some undetermined way on the initial conditions. Thus, the analysis indicates that the solution eventually oscillates about the similarity result, $\eta_f(T) = 1$, with angular frequency $\mathrm{Im}\,(\gamma_1)\,A_0$, where γ_1 is the eigenvalue with the smallest value of $|\,\mathrm{Re}\,(\gamma_1)\,|$. Unfortunately we cannot make a direct comparison between the numerical and analytical results because the a_j and b_j are unknown and the $\mathrm{Re}\,(\gamma_j)$ are equal (for $n = 0$) or nearly equal (for $n = 1$). Nevertheless, the numerical results confirm that the similarity solution is approached for large times and that the approach occurs in an oscillatory fashion in time.

6. Concluding remarks

We have shown that the known similarity solutions of the shallow-water equations representing constant-volume gravity currents in both plane and axisymmetric geometries are unique and respectively linearly stable to small plane and axisymmetric perturbations. Therefore we conclude that these solutions are the large-time limits of the solutions of the initial-value problem. The analysis also reveals that the

similarity solutions are approached in an oscillatory manner with amplitudes that decay asymptotically as $t^{-\frac{1}{2}}$ in plane flows and $t^{-\gamma}$ in axisymmetric flows, where $\gamma \approx 0.2$ (although γ is a weak function of mode number and β) indicating that the asymptotic rate of approach to similarity is fairly insensitive to the initial conditions. We solved two particular initial-value problems numerically and, although it is impossible to compare directly the quantitative results of these calculations with our analysis, the qualitative aspects compare very well.

The laboratory experiments of Huppert & Simpson (1980) and Rottman & Simpson (1983, 1984) clearly show that the length (or radius) of gravity currents resulting from fixed-volume releases eventually increase as $t^{2/(3+n)}$ as predicted by similarity theory, if the initial conditions are such that the self-similar behaviour is exhibited before viscous effects become important. Unfortunately, it is very difficult to measure experimentally the details of the approach to self-similar behaviour. The predicted oscillations about the self-similar solutions are too small to be detected in the laboratory unless very careful measurements are made. The most careful laboratory measurements of gravity-current spreading rates have been made for plane flow very recently by Emblem, Krogstad & Fanneløp (1984). Their measurements show a small oscillation of the gravity-current front velocity about the similarity solution, but the measurements are not in sufficient detail to be compared quantitatively with our asymptotic theory.

Viscous effects become important when they become comparable with the inertia of the current. By comparing order-of-magnitude estimates of these two forces for gravity currents propagating over a horizontal surface, Huppert (1982) estimates the time after release when viscous effects become important as $t_* \sim [Q^4/g'^{2(1+n)}\nu^{(3+n)}]^{1/(7+5n)}$, where ν is the kinematic viscosity of the fluid in the current. After this time the motion of the current is governed by a balance between buoyancy and viscous forces. The similarity solutions discussed in the present paper may be called intermediate asymptotics in the sense that they are valid for times large compared with the characteristic time τ but small compared with the viscous time t_*. For choices of the initial conditions such that τ and t_* are comparable, the self-similar behaviour we have described here will not be observed.

The approximate equations of motion that are valid during the viscous–buoyancy regime of the flow are those of lubrication theory. Huppert (1982) has already considered this problem, and has derived, following Barenblatt (1952), the appropriate similarity solutions that are valid for times large compared with t_*. The similarity solutions show that the length (or radius) of viscous gravity currents resulting from fixed–volume releases increase as $t^{1/(5+3n)}$, which is slower than the inertia–buoyancy spreading rate. The rate of approach to the viscous–buoyancy similarity solutions can be obtained from the results of Grundy & McLaughlin (1982), who considered the same mathematical problem in a slightly different physical context. Their calculations show that perturbation to the viscous–buoyancy similarity solutions decay as t^{-1} for both plane and axisymmetric geometries.

The authors would like to acknowledge the computational and analytic efforts of Nigel Watt in the solution of the eigenvalue problem. He was financially supported by a Carnegie Vacation Scholarship. We also thank B. R. Duffy for many helpful discussions. J.W.R. acknowledges financial support from the UK Health and Safety Executive under contract 1918/01.01.

REFERENCES

BARENBLATT, G. I. 1952 Concerning some nonstationary motions of liquid and gas in a porous medium. *Prikl. Math. Mech.* **16**, 67–78 (in Russian).

BOOK, D. L., BORIS, J. P. & HAIN, K. 1975 Flux-corrected transport II: Generalizations of the method. *J. Comp. Phys.* **18**, 248–283.

COURANT, R. & FRIEDRICHS, K. O. 1948 *Supersonic Flow and Shock Waves.* New York: Interscience.

EMBLEM, K., KROGSTAD, P. Å. & FANNELØP, T. K. 1984 Experimental and theoretical studies in heavy gas dispersion. Part I. Experiments. *Proc. IUTAM Symp. on Atmospheric Dispersion of Heavy Gases and Small Particles, Delft, The Netherlands.*

FANNELØP, T. K. & WALDMAN, G. D. 1972 Dynamics of oil slicks. *AIAA J.* **10**, 506–510.

FAY, J. A. 1969 The spread of oil slicks on a calm sea. In *Oil on the Sea* (ed. D. P. Hoult), pp. 46–63.

GRUNDY, R. E. & MCLAUGHLIN, R. 1982 Eigenvalues of the Barenblatt–Pattle similarity solution in nonlinear diffusion. *Proc. R. Soc. Lond.* A **383**, 89–100.

GUDERLEY, K. K. 1942 Starke kugelige und zylindrische Verdichtungsstösse in der Nähe des Kugelmittelpunktes bzw der Zylinderachse. *Luftfahrtforschung* 19, No. 9.

HOULT, D. P. 1972 Oil spreading on the sea. *Ann. Rev. Fluid Mech.* **4**, 341–368.

HUPPERT, H. E. 1982 The propagation of two-dimensional and axisymmetric viscous gravity currents over a rigid horizontal surface. *J. Fluid Mech.* **121**, 43–58.

HUPPERT, H. E. & SIMPSON, J. E. 1980 The slumping of gravity currents. *J. Fluid Mech.* **90**, 785–799.

MCQUAID, J. 1984 Large-scale experiments on the dispersion of heavy gas clouds. *Proc. IUTAM Symp. on Atmospheric Dispersion of Heavy Gases and Small Particles, Delft, The Netherlands.*

PENNEY, W. G. & THORNHILL, C. K. 1952 The dispersion, under gravity, of a column of fluid supported on a rigid horizontal plane. *Phil. Trans. R. Soc. Lond.* A **244**, 285–311.

ROTTMAN, J. W. & SIMPSON, J. E. 1983 Gravity current produced by instantaneous releases of a heavy fluid in a rectangular channel. *J. Fluid Mech.* **135**, 95–110.

ROTTMAN, J. W. & SIMPSON, J. E. 1984 The initial development of gravity currents from fixed-volume releases of heavy fluids. In *Proc. IUTAM Symp. on Atmospheric Dispersion of Heavy Gases and Small Particles, Delft, The Netherlands.*

SEDOV, L. I. 1959 *Similarity and Dimensional Methods in Mechanics.* London: Infosearch.

SIMPSON, J. E. 1982 Gravity currents in the laboratory, atmosphere and ocean. **14**, 213–234.

STEWARTSON, K. & THOMPSON, B. W. 1968 On one-dimensional unsteady flow at infinite Mach number. *Proc. R. Soc. Lond.* A **304**, 255–273.

STOKER, J. J. 1957 *Water Waves.* Interscience.